Termination of a Magnetized Plasma on a Neutral Gas: The End of the Plasma

C. M. Cooper and W. Gekelman

Phys. Rev. Lett. **110**, 265001 — Published 24 June 2013

DOI: 10.1103/PhysRevLett.110.265001

Termination of a magnetized plasma on a neutral gas: the end of the plasma

C. M. Cooper and W. Gekelman
University of California, Los Angeles
(Dated: April 26, 2013)

Experiments are performed at the Enormous Toroidal Plasma Device (ETPD) at UCLA to study the Neutral Boundary Layer (NBL) between a magnetized plasma and a neutral gas along the direction of a confining magnetic field. This is the first experiment to measure plasma termination within a neutral gas without the presence of a wall or obstacle. A magnetized, current-free helium plasma created by a Lanthanum Hexaboride (LaB_6) cathode terminates entirely within a neutral helium gas. The plasma is weakly ionized ($n_e/n_n \sim 1\%$) and collisional $\lambda_n << L_{plasma}$. The NBL occurs where the plasma pressure equilibrates with the neutral gas pressure, consistent with a pressure balance model. It is characterized by a field-aligned ambipolar electric field, developing self-consistently to maintain a current free termination of the plasma on the neutral gas. Probes are inserted into the plasma to measure the plasma density, flow, temperature, current, and potential. These measurements confirm the presence of the ambipolar field and the pressure equilibration model of the NBL.

A Neutral Boundary Layer (NBL) occurs wherever a magnetized plasma terminates on a neutral gas in the direction of the magnetic field without touching a solid surface. This boundary can be found in the laboratory and as aurora in nature. Hot plasma enters the system at one end while energy, momentum, and plasma density are lost at the opposite end by collisions with the neutral gas and losses across the magnetic field. The asymmetry of the system results in large thermal and pressure gradients which drive heat conduction and particle convection into the neutral gas. The plasma parameters and length are determined by transport rates and can not be determined *a priori*. The lack of well-defined boundary conditions makes modeling the NBL difficult. At a minimum, the plasma velocity along the field must go to zero by the end of the layer subject to particle, flux, and energy conservation. Both an effective model and experimental confirmation of the boundary conditions exhibited in an NBL have not yet been demonstrated.

Several experiments and simulations have been performed to characterize plasma/neutral gas dynamics along the direction of a magnetic field in systems such as gaseous divertors [1] [2] [3] [4] [5], hall thrusters [6], and studies of plasma transport [7] [8] [9]. These include pressure gradient driven flows, cross-field plasma loss rates, and characterization of plasma/neutral gas dynamics. However, the final boundary condition of the plasma in these studies is always Bohm sheath to a solid object, bypassing the physics of the NBL. Neutral Boundary Layers occur in nature as aurora where a magnetized plasma in space terminates on objects cool and massive enough to have an atmosphere [10] [11] [12]. Energetic particles create and heat plasma [13] that eventually thermalizes and recombines through interactions with the neutral gas[14] [15] [16].

In this letter, we report the first direct measurements of the structure within a plasma terminating on a Neutral Boundary Layer. The ambipolar electric field terminating the plasma is measured and pressure equilibration is confirmed as the criteria for plasma termination. The experiment is conducted at the Enormous Toroidal Plasma Device (ETPD) at UCLA [17] wherein a magnetized column of helium plasma created by a LaB_6 source terminates on a neutral helium gas without touching the machine wall. Direct measurements of the plasma parameters are made throughout the boundary to characterize the physics of the NBL. A three fluid plasma transport model is used to characterize the NBL and is compared to the measurements.

The NBL occurs where the plasma pressure $p_p = n_e k_B(T_e + T_i)$ equals the neutral gas pressure $p_n = n_n k_B T_n$, defined as the termination point. Beyond this point, electrons and ions convected into the system collisionally come to rest. Due to their lighter mass, electrons collisionally damp their momentum much faster than the ions. An ambipolar electric field develops self-consistently to drag the electrons through the neutral gas at the ion velocity to prevent charge buildup in the NBL. The electric field acts like a sheath extending into the neutral gas, regulating the electron and ion fluxes on their charge separation scales. For a typical Bohm sheath on a solid body, an ambipolar electric field develops on the electron Debye length scale, λ_D to prevent a current. In the Neutral Boundary Layer, the electric field develops on the neutral collision length $\lambda_n = 1/n_n\sigma_n$ with a collisional cross section σ_n to prevent a current. The length of the measured electric field is 1 m $\sim 50\lambda_n \sim 10^5\lambda_D$.

A schematic of the ETPD and the measurement locations are shown in Fig. 1. The ETPD is a toroidal basic plasma research device 3 m tall, 2 m wide with a 5 m major radius. The device is evacuated then backfilled with 3.6 mTorr of helium gas. A 20 cm x 20 cm thermally emissive plate of Lanthanum Hexaboride (LaB_6) is biased 210 V with respect to a semi-transparent molybdenum anode mesh 1.6 m away, both oriented along the magnetic field. The emitted electrons ionize the gas to

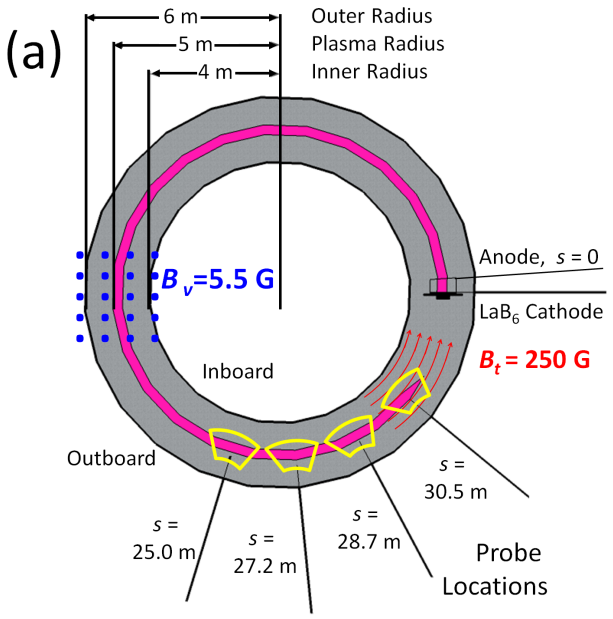

FIG. 1. (Color online) A schematic of the ETPD setup showing the helium plasma transiting around the machine one time and terminating on the background helium gas. Data planes (yellow) are taken in the last 800 cm of the plasma. Data are recorded at 1300 locations on each of the 4 the arc shaped planes.

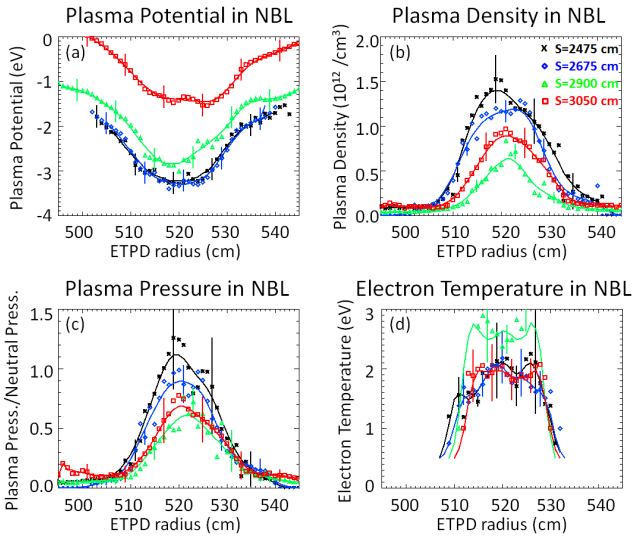

FIG. 2. (Color online) Radial profiles of (a) plasma potential, (b) plasma density, (c) plasma pressure normalized to neutral pressure, and (d) electron temperature in four locations in the NBL. Smoothed profiles are plotted over the points to guide the eye and locate the center maximums. T_e could not be reliably determined outside the plasma column.

make a plasma which extends < 30 m past the anode then heats it. A toroidal magnetic field $B_t = 250$ G and a vertical magnetic field $B_v = 5.5$ G confine the plasma to a helical geometry, rising 75 cm every 3140 cm revolution of the machine. The spatial coordinates r and s are the radial coordinate and the distance along the magnetic field at the center of the plasma at $r = 520$ cm, with the anode at $s = 0$.

The plasma temperature and density are measured with a Langmuir probe calibrated with a 96 GHz microwave interferometer [18] [19] [20]. The plasma velocity is measured using a Mach probe [19] and the plasma potential is measured using an emissive probe [21]. The data are recorded on arc shaped planes oriented to follow the rising magnetic field lines in the machine locations at the four locations shown in Fig. 1. The axial and radial profiles of the plasma parameters are determined from the data planes and used to calculate the equilibrium transport and force balance.

The radial profiles of the plasma parameters at the four toroidal locations are plotted in Fig. 2. The first two locations ($s = 2475$ cm, black x and $s = 2675$ cm , blue diamond) are upstream of the NBL. The third location ($s = 2900$ cm, green triangle) is at the beginning of the NBL and the fourth location ($s = 3050$ cm, red square) is at its end. The plasma potential (a) profiles are unchanged upstream but change in the NBL electric field. The plasma density (b) decreases due to radial losses until the last location where a small increase can be seen due to ionization in the NBL. The plasma pressure normalized to the fill pressure (c) drops due to density losses until the NBL. The electron temperature (d) remains below the threshold for ionization (2 eV) except in the NBL where Ohmic heating occurs. Ionization rapidly cools the plasma by the end of the NBL. Outside of the plasma, T_e was extremely low (0.5 eV) and difficult to consistently measure due to the low density. The error bars represent the goodness of fit from analysis and the statistical fluctuation of the 20 ensemble-averaged measurements at each location.

The experiment is performed in the weakly ionized limit, $n_e/n_n \sim 1\%$ where collisions with the neutral gas dominate the physics $\nu_{\alpha n} = n_n \sigma_{on}(k_B T_\alpha / m_\alpha)$. To simplify the analysis, several assumptions are made about the density, velocity, and temperature of the three fluids.

a) The neutral gas in the NBL is a stationary with a temperature $T_n = 300$ K and a density $n_n = n_{n,wall} = 1.16 \times 10^{14}$ cm^{-3} as measured by a vacuum gauge.

b) The ions are assumed to be in thermal equilibrium with the neutral gas ($T_i = T_n$).

c) The plasma is current free ($\mathbf{v_e} = \mathbf{v_i} = \mathbf{v_p}$).

The plasma current in the NBL was calculated from measured volumetric magnetic field data taken with a magnetic pickup coil probe [23]. The axial plasma current in the NBL was small ($v_{is} \sim 0.9 v_{es}$) and trending towards zero. The current was not related to the NBL electric field and can be explained by a modified ambipolar closure current scheme.

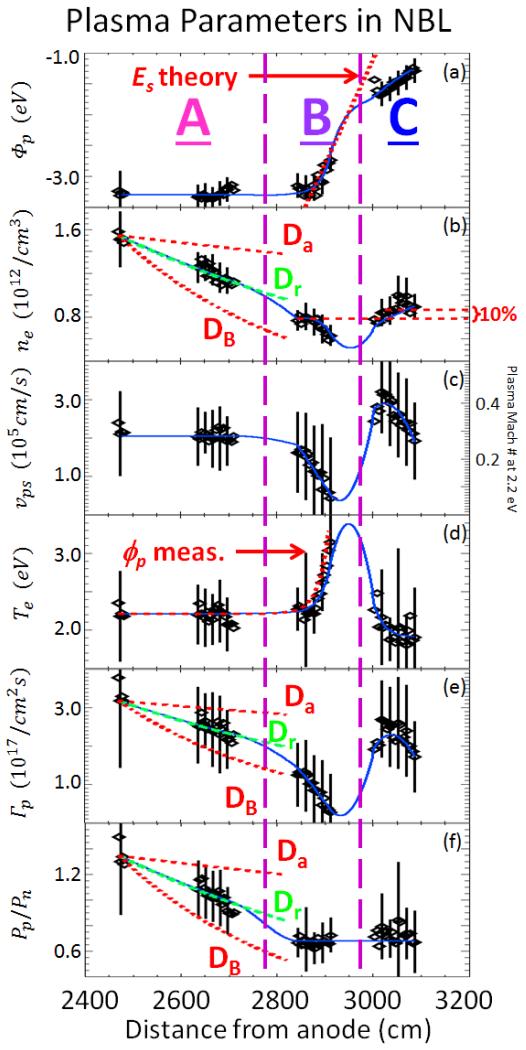

FIG. 3. (Color online) axial profiles of (a) the plasma potential with the predicted electric field (dashed, red), (b) the plasma density and the predicted 10% bump in density (dashed, red), (c) the plasma flow speed, (d) electron temperature with Φ_p (dashed, red) to show Ohmic heating, (e) the axial plasma flux, and (f) the plasma pressure normalized to neutral pressure in the NBL. In (b), (e), and (f) the profiles predicted by classical and Bohm diffusion (D_a and D_B dashed, red) are compared to the calculated diffusion (D_r, dashed, green). Smoothed profiles (blue) are plotted to guide the eye. Zones A, B, and C show the pre-NBL, early NBL, and the end of the NBL.

The axial profiles of the plasma parameters in Fig. 3 are generated by interpolating the data planes onto the center of the plasma. The plasma potential Φ_p (a) suggests that the data be divided into three zones. Zone A is upstream of the NBL and has no electric field. The plasma is far from the source heating and too cool for ionization or conductive losses and T_e is constant. Radial losses along the column create an axial pressure gradient $\partial p_e/\partial s$ which is balanced by a collisional neutral drag and determines v_{ps}. The plotted v_{ps} is calculated using the locally measured Mach number $M = v_{ps}/c_s$ and plasma sound speed $c_s = (k_B T_e/m_i)^{1/2}$. Using a flux conservation model with a constant axial velocity and assuming diffusive radial losses $\nabla_\perp(n_e v_{p\perp}) = D_r n_e/R_p^2$ where R_p is the radius of the plasma, $\partial n_e/\partial s = -n_e D_r/v_{ps} R_p^2$. The radial diffusion coefficient determined from the measured axial density profile is $D_r = 2.7\times10^4$ cm^2/s. This is half the theoretical Bohm diffusion coefficient $D_B = ck_BT/16eB = 5.5\times10^4$ cm^2/s but four times the classical current-free ambipolar diffusion coefficient in the weakly ionized limit $D_{a,\perp} = (T_i+T_e)D_{e,\perp}D_{i,\perp}/(T_iD_{e,\perp}+T_eD_{i,\perp}) = 6.9\times10^3$ cm^2/s where $D_{\alpha,\perp} = (k_BT_\alpha/m_\alpha\nu_{\alpha n})(\nu_{\alpha n}^2/(\nu_{\alpha n}^2+\omega_{c\alpha}^2))$ is the cross field diffusion rate for each species α.

The termination electric field begins in zone B where the plasma collisionally comes to a rest. The spatial extent of the electric field is longer than λ_n but shorter than the energy loss length in this zone. The electrons isotropize kinetic energy without losing thermal energy and $k_B\partial T_e/\partial s \sim e\partial\Phi_p/\partial s$. This is seen in Fig. 3 (d) where $e\Phi_p(s)$ is plotted as a dashed red line.

In zone C, the electric field decreases as the plasma potential approaches zero. Interestingly, Ohmic heating and plasma deceleration lowers the ionization length $<$ 10 cm. Ionization begins anew, and the plasma cools back below the ionization threshold by the end of the NBL. The potential energy density gained by the plasma in the NBL, $n_e\Delta\Phi_p = 2.5n_e$ eV/cm^3, is equal to the energy lost to ionizing additional density, $\Delta n_e E_{ionz,He} = 24.6\Delta n_e$ eV/cm^3. The corresponding rise in density is observed $\Delta n_e/n_e = \Delta\Phi_p/(E_{ionz,He}+T_e) = 10\%$. The additional ionization drives the axial flow seen in zone C. Once ionization has subsided, the flow damps to zero at the same rate in zone B.

Fig. 4 shows a 2D colorplot of Φ_p interpolated into toroidal coordinates (r, s). The gradient of Φ_p i.e. the electric field is plotted as arrows. The isopotentials form "nested U's" indicating a 3-D ambipolar field. The field-aligned component of the electric field is multiplied by 10 to clearly show the termination electric field.

The properties of the equilibrium NBL can be approximated by using a three-fluid collisional transport model. The Braginskii steady state momentum equation [24] for the electrons and ions in the presence of a neutral gas are subtracted to produce a generalized Ohm's Law. Neglecting terms of order m_e/m_i and T_i/T_e yields an equation relating the pressure gradient and the drag in the plasma along the direction of the confining field $\hat{s}$,

$$\frac{\partial p_e}{\partial s} = -en_eE_s - \Theta n_e k_B\frac{\partial T_e}{\partial s} - m_e n_e v_{ps}\nu_{en} \qquad (1)$$

Where $\Theta = t_n + 0.71$ is the coefficient for the thermal force in the direction of the field, 0.71 from electron-ion collisions and t_n from electron neutral collisions. Eq.

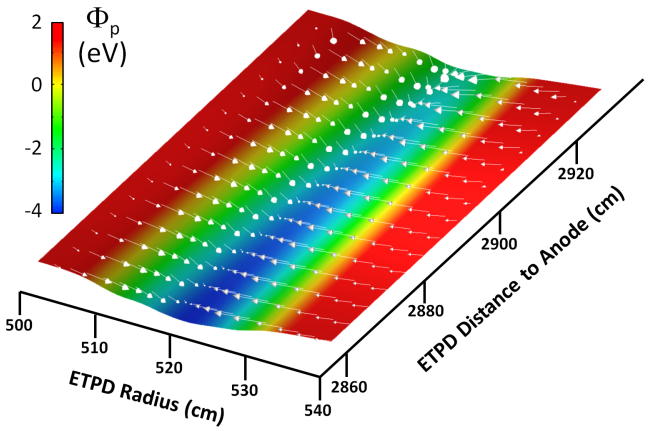

FIG. 4. (Color online) Plasma potential forming isopotential "nested U's" in the NBL. The arrows are the calculated electric field with the field aligned component multiplied by 10 to accentuate the parallel electric field terminating the plasma.

1 can be simplified in zone B of the ETPD NBL using $k_B\partial T_e/\partial s = e\partial\Phi_p/\partial s = -eE_s$, and $\partial p_e/\partial s = 0$. This yields a formula for the electric field E_s required for current-free termination of a plasma at an axial velocity v_{ps},

$$E_s = \frac{v_{ps}m_e\nu_{en}}{e(1-\Theta)} = \frac{J_e}{(1-\Theta)\sigma_{en}} = \frac{-J_i}{(1-\Theta)\sigma_{en}} \quad (2)$$

The electric field drives an electron flux $\Gamma_e = \Gamma_i$ such that $J_{tot} = 0$ subject to a modified weakly ionized plasma conductivity $(1-\Theta)\sigma_{en}$. Lacking axial profiles of the neutral density and momentum, Eq. 2 is used to calculate a zero-dimensional approximation for the termination electric field using the slowly varying plasma parameters in zone B and the undepleted, stationary, neutral fill density. This is compared to changes in Φ_p computed across regions with the same offset due to the presheath and sheath, $\sim 2T_e$ [22]. The finer axial dependence of the termination electric field suggested by the data can only be realized through collisional transport codes. The value of this electric field for $t_n = 0.1$ is plotted in the top panel of Fig. 3 and agrees well with the observed electric field.

Adding the electron, ion, and neutral gas axial momentum equations yields,

$$\frac{\partial}{\partial s}(p_p + p_n) = -m_i\left(v_{ps}\nabla_\perp\Gamma_{p,\perp} + v_{ns}\nabla_\perp\Gamma_{n,\perp}\right) \quad (3)$$

The plasma is in an axial pressure equilibrium with the neutral gas subject to the radial losses $\nabla_\perp\Gamma_\perp$. The total pressure $p_p + p_n$ found by integrating Eq. 3 is not constant along the field and explains $p_p > p_{n,fill}$ as observed upstream of the NBL. The relative diffusivities are ordered $D_{a,||} >> D_n = T_n/m_n(\nu_{nn} + \nu_{ni}) >> D_{a,\perp}$

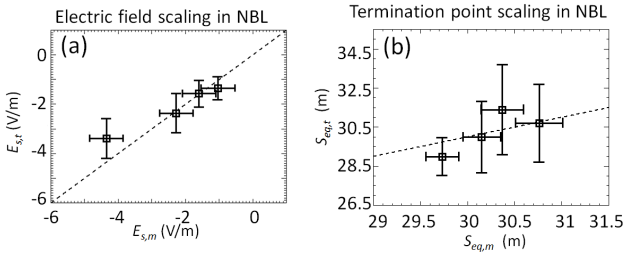

FIG. 5. (left) The measured vs. predicted NBL electric field (right) and termination point over a scaling of plasma parameters.

. This implies that plasma pressure convects the neutral gas out along the field while cross field diffusion slowly fills it back in, maintaining a depleted neutral gas pressure inside the column. For $p_p > p_{n,fill}$ upstream, the plasma can push the neutral gas out of the way but for $p_p < p_{n,fill}$ in the NBL, the neutral gas terminates the plasma.

The experiment was repeated, varying the input plasma power $P_{dis} = I_{dis}V_{dis}$ measured from the anode-cathode discharge current and voltage. This created a scaling of n_e and v_{ps} in the NBL and shifted the plasma termination point, while T_e stayed constant below the ionization threshold ($\sim$ 2 eV). The measured axial profiles were similar to those in Fig. 3. The plasma parameters were measured in the pre-NBL area in zone A and Φ_p was measured throughout the NBL. The measured electric field, $E_{s,m}$ is compared to $E_{s,t}$ predicted by Eq. 2 in the left panel of Fig. 5. A value of $t_n = 0.1$ again fits the data the best, representing a small correction to the electron-ion thermal force. The location of the $E_{s,m}$, $s_{eq,m}$, is compared to the location for pressure equilibration, $s_{eq,t}$, in the right panel of Fig. 5. The location of the termination point was calculated by extrapolating the plasma pressure, $p_p(s) = p_p(s_o)e^{\frac{D_r}{v_{ps}R_p}(s-s_o)}$ using D_r previously measured. The predicted pressure equilibration termination point was found by setting $p_p(s_{eq,t}) = p_n$ agrees well with the measured electric field location $s_{eq,t}$.

In conclusion, the ambipolar electric field terminating the plasma in a Neutral Boundary Layer was measured for the first time and agreed well with a three fluid collisional plasma model. The NBL was observed to occur where the plasma pressure equaled the neutral gas pressure, supporting a pressure balance model for termination. Good agreement was found repeating both measurements over a scaling of plasma parameters. The NBL is relevant in auroral termination where ambipolar sheaths must be established to maintain particle fluxes subject to the different motilies of electrons and ion species colliding with the neutral gases. The $\sim$ 10 km termination region of the aurora at an altitude of $\sim$ 100 km is $\sim 10^3\lambda_n \sim 10^7\lambda_D$, several collision lengths

longer than the ETPD NBL due to the additional NBL ionization from high energy auroral electrons[25]. Additionally, the presence of neutral molecules in an auroral NBL, such as in the Earth's thermosphere, thermalize T_e more effectively through excitation of rotational and vibrational states. In situ measurements of the local axial flow and electric field in the termination region are needed and its altitude should be compared to the pressure and auroral energy density (q_e) equilibration altitude, $(p_p + q_e) = p_n$. Theoretical axial profiles of NBL plasma parameters in this work, including the depleted neutral density, can only be predicted by a multidimensional plasma transport simulation and will be published in a future paper.

The authors would like to acknowledge the valuable contributions of Patrick Pribyl, Zoltan Lucky, and Marvin Drandell for their helpful discussions and technical expertise, and Jim Maggs and George Morales for their insight and expertise on plasma transport. This work was performed at the Basic Plasma Science Facility at UCLA, supported by a cooperative agreement between the National Science Foundation and the Department of Energy.

[1] L. Schmitz, R. Lehmer, G. Chevalier, G. Tynan, P. Chia, R. Doerner, and R. Conn, J. Nucl. Mat. **176-177**, 522 (1990).

[2] L. Schmitz, B. Merriman, L. Blush, R. Lehmer, R. W. Conn, and A. Grossmhn, Phys. Plasmas **2** (1995).

[3] D. Stotler and C. Karney, Contrib. Plasma Phys. **34**, 392 (1994).

[4] W. Schneider, D. B. Heifetz, K. Lackner, J. Neuhauser, and D. E. Post, J. Nucl. Mat. **121**, 178 (1984).

[5] G. Matthews, J. Nucl. Mat. **220-222**, 104 (1995).

[6] E. Ahedo, P. Martnez-Cerezo, and M. Martnez-Sanchez, Phys. Plasmas **8**, 3058 (2001).

[7] A. Fruchtman, G. Makrinich, and J. Ashkenazy, Plasma Sources Sci. Tech. **14**, 152 (2005).

[8] A. Fruchtman, Plasma Sources Sci. Tech. **18**, 025033 (2009).

[9] J.-L. Raimbault, L. Liard, J.-M. Rax, P. Chabert, A. Fruchtman, and G. Makrinich, Phys. Plasmas **14**, 013503 (2007).

[10] G. Paschmann, S. Haaland, and R. Treumann, *Auroral Plasma Physics* (Kluwer Academic, Dordrecht, 2003) p. 44.

[11] C. Russell, Planetary and Space Science **53**, 473 (2005).

[12] M. Kivelson, Adv. Space Res. **33**, 2061 (2004).

[13] M. H. Rees, Planetary and Space Science **11**, 1209 (1963).

[14] M. Kivelson and C. Russell, *Introduction to Space Physics* (Cambridge, 1996).

[15] A. E. Hedin, J. Geo. Res. **96**, 1159 (1991).

[16] R. Roble and M. Rees, Planetary and Space Science **25**, 991 (1977).

[17] C. M. Cooper, W. Gekelman, P. Pribyl, and Z. Lucky, Rev. Sci. Instrum. **81**, 083503 (2010).

[18] F. F. Chen, *Plasma Diagnostic Techniques* (Acad. Press, 1965) p. Chap. 4.

[19] I. Hutchinson, *Principles of Plasma Diagnostics* (Cambridge, 2002).

[20] I. G. Brown, A. B. Compher, and W. B. Kunkel, Phys. Fluids **14**, 1377 (1971).

[21] R. F. Kemp and J. M. Sellen, Rev. Sci. Instrum. **37**, 455 (1966).

[22] J. P. Sheehan, Y. Raitses, N. Hershkowitz, I. Kaganovich, and N. J. Fisch, **073501**, 1 (2011).

[23] E. T. Everson, P. Pribyl, C. G. Constantin, A. Zylstra, D. Schaeffer, N. L. Kugland, and C. Niemann, Rev. Sci. Instrum. **80**, 113505 (2009).

[24] S. I. Braginskii, *Transport Processes in a Plasma* (1965).

[25] J. C. G. Walker and M. H. Rees, Planet. Space Sci. **16**, 459 (1968).